



Two-dimensional polymorphism and melting in a monolayer of nitric oxide adsorbed on graphite

J.P. Coulomb, J. Suzanne, M. Bienfait, M. Matecki, A. Thomy, B. Croset, C. Marti

► To cite this version:

J.P. Coulomb, J. Suzanne, M. Bienfait, M. Matecki, A. Thomy, et al.. Two-dimensional polymorphism and melting in a monolayer of nitric oxide adsorbed on graphite. *Journal de Physique*, 1980, 41 (10), pp.1155-1164. 10.1051/jphys:0198000410100115500 . jpa-00208942

HAL Id: jpa-00208942

<https://hal.science/jpa-00208942>

Submitted on 4 Feb 2008

HAL is a multi-disciplinary open access archive for the deposit and dissemination of scientific research documents, whether they are published or not. The documents may come from teaching and research institutions in France or abroad, or from public or private research centers.

L'archive ouverte pluridisciplinaire **HAL**, est destinée au dépôt et à la diffusion de documents scientifiques de niveau recherche, publiés ou non, émanant des établissements d'enseignement et de recherche français ou étrangers, des laboratoires publics ou privés.

Classification
Physics Abstracts
61.12 — 68.20

Two-dimensional polymorphism and melting in a monolayer of nitric oxide adsorbed on graphite (*)

J. P. Coulomb, J. Suzanne, M. Bienfait, M. Matecki ⁽¹⁾
A. Thomy ⁽²⁾, B. Croset ⁽³⁾ and C. Marti ⁽³⁾

Département de Physique, Faculté des Sciences de Luminy, 13288 Marseille Cedex 2, France.

(Reçu le 3 mars 1980, accepté le 3 juin 1980)

Résumé. — Trois solides bidimensionnels (2D) γ , δ , β , sont observés à basse température par diffusion de neutrons dans une monocouche d'oxyde nitrique adsorbé sur du graphite. La structure de deux de ces solides, γ et β , est déterminée. Dans les deux cas, les molécules d'oxyde nitrique sont dimérisées, mais dans la phase β les molécules N_2O_2 sont debout, tandis que dans le solide γ elles sont couchées sur le substrat. Les configurations β et γ sont analogues à l'empilement de deux plans de l'oxyde nitrique massif ; il s'agit du plan (001) pour la phase β et du plan (10 $\bar{1}$) pour le solide γ . La structure δ intermédiaire n'est pas résolue mais une maille est proposée. Si on augmente la température, les solides 2D fondent. On s'attache particulièrement à l'étude de la transition β -liquide qui s'avère être du premier ordre. D'autres transitions du premier ordre sont aussi observées comme les transformations $\beta \rightleftharpoons \delta$, liquide \rightleftharpoons gaz et $\gamma \rightleftharpoons$ gaz. Tous ces résultats, ainsi que des mesures d'isothermes d'adsorption obtenues précédemment, sont rassemblés dans un diagramme de phase 2D qui présente trois points triples, une température critique et un point tricritique.

Abstract. — Three two-dimensional (2D) solids γ , δ and β have been observed at low temperature by neutron scattering in the first monolayer of nitric oxide adsorbed on graphite. The structure of two of these solids, γ and β , has been determined. In both cases, nitric oxide molecules are dimerized, but in the β phase N_2O_2 molecules stand up whereas in the γ solid they lie down on the substrate. The β and γ configurations are analogous to the packing of two planes of the nitric oxide bulk crystal namely the (001) plane for the β phase and the (10 $\bar{1}$) plane for the γ solid. The intermediate δ structure is not resolved but a possible unit cell is given. Increasing the temperature results in a melting of the 2D solids. A particular emphasis is made on the β -liquid transition which is shown to be first order. Other first order transitions are also observed like the β solid \rightleftharpoons δ solid, liquid \rightleftharpoons gas and γ solid \rightleftharpoons gas transformations. All these results combined with previous adsorption isotherm measurements are put together in a proposed 2D phase diagram displaying three triple points, one critical temperature and one tricritical point.

1. Introduction. — Physisorbed monolayer films give good examples of quasi two-dimensional (2D) phases. The weak Van der Waals adsorbate-adsorbate and adsorbate-substrate interactions allow one to observe the various states of 2D matter under equilibrium conditions in a convenient temperature and pressure range.

In spite of the numerous studies performed up to now [1, 2, 3], several problems remain unsolved. In particular, the solid-solid (polymorphism) and the

solid-liquid (melting) transitions are not well understood.

Concerning the solids, the question whether the structure of the adsorbed layer is similar to that of the densest plane of bulk solid has only been solved in a few cases. For instance, the rare gases adsorbed on graphite exhibit a hexagonal structure showing a commensurate-incommensurate transition [4, 5] induced by the periodic substrate field which has no equivalent in three dimensions for those systems. When the molecule of adsorbate becomes more complicated, one is expecting various configurations depending on concentration, temperature and substrate field. *A priori*, one does not know to what extent they resemble the bulk configurations. This problem begins to be investigated in the case of simple molecules O_2 , N_2 , C_2D_6 , NO adsorbed on graphite (0001). Oxygen

(*) Experiments performed at I.L.L.

⁽¹⁾ Université de Rennes, Laboratoire de Chimie Minérale, D-35031 Rennes.

⁽²⁾ Laboratoire M. Letort, C.N.R.S., 54600 Villers-Les-Nancy, France.

⁽³⁾ Institut Laue-Langevin, 38042 Grenoble, France.

exhibits 2D phases analogous to that of bulk [6]. An antiferromagnetic ordering occurs at low temperature. As for N_2 molecules, an orientational ordering takes place below 30 K. Above this temperature, molecules are free to rotate at the 2D lattice points [7]. For C_2D_6 , an orientational ordering also disappears above a transition temperature [8]. Finally preliminary results have been published on the polymorphism of NO adsorbed on graphite [9]. The molecule is dimerized and can stand up or lie down on the substrate according to coverage and temperature. One of the goals of this paper is to complete and develop this previous study.

Other problems concerning the 2D liquids have raised longstanding debates about the order of the melting transition. Depending on the theoretical model, the melting can be a sharp (first order) or continuous (higher order) transition [10, 12]. It has been extensively studied experimentally with numerous adsorbates using graphite as a substrate [8, 9, 13-26]. The results indicate that solid-fluid transitions are more or less abrupt depending on the system. When the transition is continuous, one does not know if it is due to an intrinsic property of the melting of the layer or a broadening produced by surface heterogeneities or size effects [22]. For instance, several authors believe that the melting of a submonolayer of krypton adsorbed on graphite is continuous [24, 39]. However, this result is questioned by others [40, 41] who claim that this transition is first order.

The problem of melting in two dimensions is still hot although significant progress have been achieved recently [3]. We want here to bring an experimental contribution to this subject in showing that a first order melting transition occurs in a submonolayer of NO adsorbed on graphite.

All these results concerning 2D polymorphism and melting are summarized on a very rich phase diagram showing among other features three triple points, one critical temperature and one tricritical point.

The NO/graphite system has been studied in detail by Matecki, Thomy and Duval (MTD), using adsorption volumetry [27, 28] between 78 and 92 K ($6 \times 10^{-4} < p < 6$ torrs). The main results are represented schematically in figure 1 in a $x(p)$ diagram where x is the coverage and p the vapour pressure surrounding the sample. Below 87 K, the 2D critical temperature, the adsorption isotherms exhibit during the formation of the first layer, two vertical substeps due to two successive first order transitions. The first one would represent an equilibrium between a 2D gas and a 2D condensed phase called α whose dimerized N_2O_2 molecules could lie down on the graphite surface. MTD could not decide whether this α phase is a 2D liquid or a 2D solid. The second transition called $\alpha \rightleftharpoons \beta$ might correspond to a transformation from the solid (or liquid) α with lying down molecules into a solid β with standing up molecules. The analysis of the adsorption volumetry results does not allow to settle those questions. Furthermore, the extrapola-

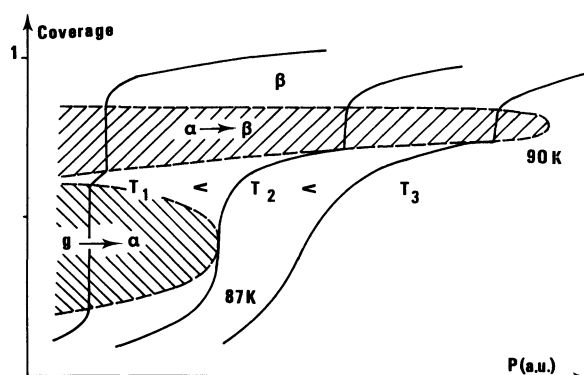


Fig. 1. — Schematic representation of the adsorption isotherm measurements of Matecki, Thomy and Duval [27, 28]. Two successive first order transitions $g \rightleftharpoons \alpha$ and $\alpha \rightleftharpoons \beta$ were observed. The nature of the α and β condensed phases was unknown.

tion towards low temperatures suggests, according to MTD, a triple point at 15 K, a temperature far down from the lowest temperature they studied, making the validity of this extrapolation questionable.

All these difficulties can be overcome by using neutron diffraction. With neutrons, the structural studies can be carried out whatever the vapour pressure surrounding the surface is. This is an advantage of prime importance knowing that adsorption volumetry and LEED are inefficient below 10^{-5} and above 10^{-4} torr respectively. Furthermore, in contrast to LEED, multidiffraction effects are totally negligible with neutrons and the diffraction patterns can be interpreted more easily.

2. Experimental procedures and characterization. —

The small interaction cross section of neutrons with molecules requires to use powders to increase the surface to bulk ratio and thus obtain a signal due to the adsorbed phases. We chose papyex [29], a recompressed exfoliated graphite having a large volumic adsorption area ($\sim 22 \text{ m}^2/\text{g}$, 1.1 g/cm^3) predominantly of basal plane (0001) surfaces, with mean orientation parallel to the plane of the sheet. It has been used previously for neutron or X-ray scattering of films [8, 9, 30-32]. Papyex is a manufactured product similar to grafoil which was extensively used in adsorption studies [1, 13, 15, 16, 20-22, 24].

After an outgassing of the substrate at 800°C for 24 h an adsorption isotherm was measured at 77.3 K in order to calibrate the adsorbed quantity and to check the papyex surface qualities. It is drawn on figure 2 and compared to that obtained on exfoliated graphite. We still observe two substeps but the second one is no longer vertical. That is due to imperfections on the papyex surface; those imperfections can either create an adsorption energy distribution or limit the size of the 2D adsorbed crystallites inducing a variation $\Delta\mu$ of the chemical potential in the layer. Nevertheless, μ varies only by about 6 cal./mole, a value, deduced from the pressure variation, much

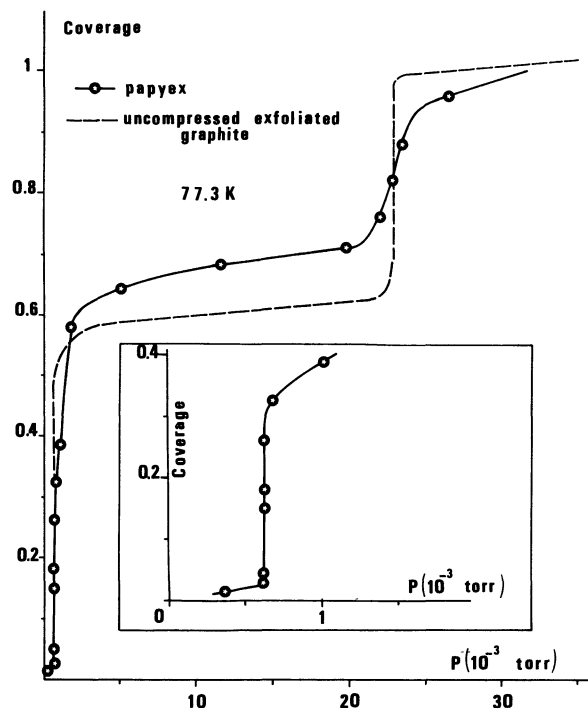


Fig. 2. — Adsorption isotherms of NO on graphite at $T = 77.3$ K. Compression of exfoliated graphite (i.e. papyex) produces inhomogeneities responsible for the non verticality of the second step and the larger slope of the plateau between steps. Nevertheless, because of its large density and preferential orientation, papyex is necessary to carry out neutron experiments. Monolayer completion corresponds to an adsorbed volume $V_a = 12.5$ cm³ STP/g for a specific area of 22 ± 1 m²/g.

smaller than the adsorption energy (~ 4500 cal. mole⁻¹) of NO on graphite [27]. Such a minor variation of the chemical potential does not probably modify the nature of the adsorbed phases.

The adsorption cell used in our neutron experiments contains 20.4 g of papyex. Coverage $x = 1$ corresponds to an adsorbed quantity of 12.5 cm³ STP/g, i.e. an area of 12 Å² per N₂O₂ molecule. A liquid helium cryostat allows us to achieve a temperature regulation at ± 0.1 K. Careful experimental procedures have been used to reach equilibrium upon adsorption. The layer was always annealed. Reproducibility or reversibility tests were carried out.

The experiments were performed at Institute Laue-Langevin (I.L.L.) in Grenoble on the two axis diffractometers D1B and D2, using respectively wavelength $\lambda = 2.516$ Å and $\lambda = 1.21$ Å. Neutron spectroscopy of adsorbed phases is now a routine technique. The reader interested in the detailed procedures can refer to the paper by Kjems *et al.* [33].

Our recorded diffraction patterns strongly depends on coverage and temperature. Some of them corresponds to 2D solids, others show evidence of 2D liquids. They are thoroughly analysed in the following sections. Three different solid structures appear. They can exist alone (single-phase domain) or coexist (two-phase domain). Fluids can appear alone or

coexist with a solid as well. The next section deals with the 2D solids and 2D polymorphism. Then, 2D fluids and melting are investigated. Finally, a tentative phase diagram of NO adsorbed on graphite is presented.

3. 2D Polymorphism. — **3.1 DIFFRACTION PATTERNS.** — Typical Debye Scherrer patterns of NO adsorbed on graphite are given in figure 3. The measurements are carried out at 10 K for three different coverages 0.4, 0.85 and 1.05. It is clear that the patterns depend strongly on coverage x . At $x = 1.05$ (Fig. 3a), a main peak occurs near the scattering angle $2\theta = 44^\circ$. It is followed by a small peak around 60° and by a bump near 85° . The two peaks have the sawtooth characteristic shape of the diffraction by a powder of

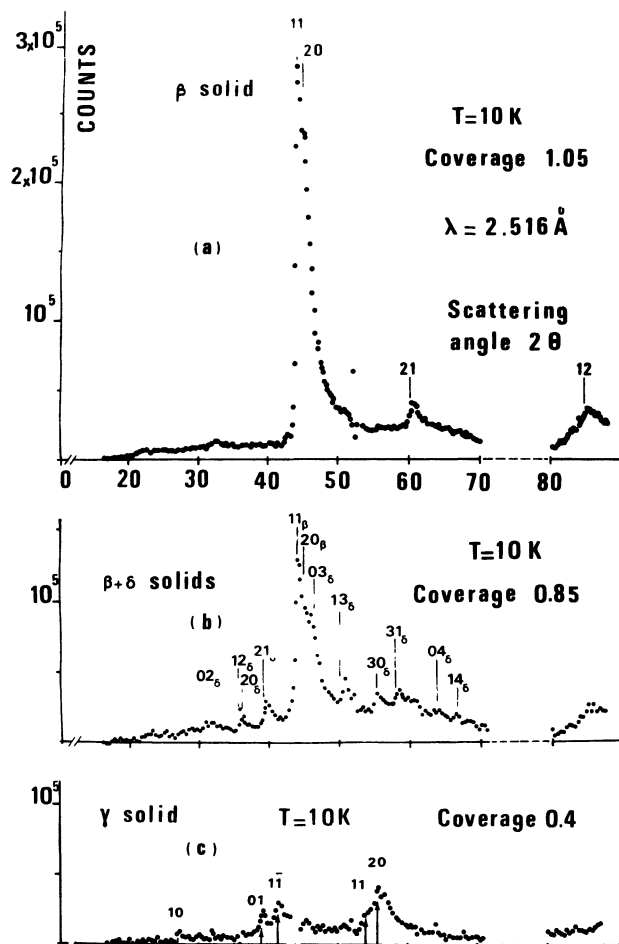


Fig. 3. — Neutron diffraction patterns from NO adsorbed on graphite at 10 K and three different coverages ($\lambda = 2.516$ Å). Background scattering from the substrate has been subtracted. Typical background level is 5×10^5 counts for the present experimental conditions. All curves are normalized to the same number of incident neutrons. The dashed lines on the abscissa correspond to the position of the substrate peaks. *Blind* windows correspond to the substrate peak modification due to the overlayer : (002) peak at 44° ; (100) and (101) peaks between 72 and 80° (dashed lines on the abscissa). a) β solid; coverage $x = 1.05$; b) coexistence of β and δ solids; $x = 0.85$; c) γ solid; $x = 0.4$. The arrows indicate the positions and the relative intensities of Bragg peaks from the N₂O₂ layer, according to the model drawn in figure 8.

planes [33, 34]. The pattern of figure 3a persists up to 74 K and thus corresponds to the β phase of MTD. At $x = 0.4$ (Fig. 3c), the diffraction is quite different. Several little peaks are visible around 40 and 55°. They define a new solid phase that we call γ [9]. This low temperature phase could not be observed by MTD since they performed their adsorption isotherm measurements above 78 K, a temperature where γ is no longer stable. The observation of this new phase is inconsistent with the assumption of a triple point at 15 K because we should record at $x = 0.4$ a β solid (coexisting with a 2D gas). The phase diagram is more complex than expected. This point will be analysed in 5. At $x = 0.85$, a third diffraction pattern occurs. It exhibits a large peak at $\sim 44^\circ$ which can be attributed to the β phase, and other peaks between 35 and 40° and 50 and 60° which do not correspond to any to those observed in the β and γ solids. Thus, a new solid phase occurs at $x \approx 0.85$ and $T = 10$ K and coexists with the β phase. We call it δ . Besides one can find a coverage where this δ solid occurs alone as indicated by the diffraction pattern obtained at $x = 0.65$ and 10 K and represented in figure 4.

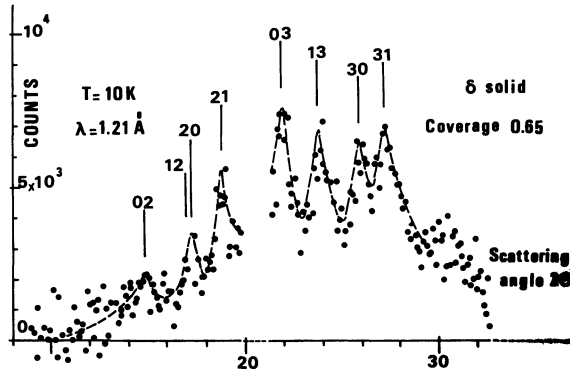


Fig. 4. — Same as figure 3 but with $\lambda = 1.21$ Å, $x = 0.65$ and a shorter counting time. The δ solid occurs alone. The dashed line is a guide to the eye.

3.2 INTERPRETATION. — **3.2.1 Unit cells.** — Firstly, the 2D unit cells of the three β , γ and δ solids are determined by indexing the different diffracted beams. A systematic computation using the following method is carried out to solve this problem. We index the first three peaks with simple indexes hk . Then, we calculate the cell parameters a , b , (a, b) and the scattering position of the other peaks. The computation is repeated for all the hk pairs with $|h|, |k| < 5$. Among the various possible solutions, we choose the smallest unit cell permitting to index all the observed diffracted beams. The results are given in table I. The β unit cell is slightly different from that previously published by the same authors in a letter [9] ($a = 6.54$ Å; $b = 3.87$ Å). Here we perform a careful analysis of the peak shape (see 3.2.3) and use the parameters of the fit to deduce the β unit cell. The

Table I.

	a	b	(a, b)
β	6.58 ± 0.08	3.90 ± 0.04	90°
δ	8.1 ± 0.6	9.5 ± 0.7	90°
γ	5.60 ± 0.04	3.88 ± 0.04	$105^\circ \pm 1$

experimental uncertainty is estimated to be about $\Delta\theta = \pm 0.1^\circ$. The resulting errors on a and b are given in the table.

We notice that all the cells are incommensurate with the (0001) graphite plane. Two of them are rectangular and the other is oblique.

3.2.2 Structure. — As recalled in the introduction, neutron diffraction has the main advantage to obey the kinematic theory of diffraction. If one disposes of enough diffraction peaks, one can, in principle, determine the crystal structure from the peak intensities. The standard theory of the diffraction applied to 2D crystals having a preferential orientation was adapted by Kjems *et al.* [33] from Warren formalism [34]. Readers not familiar with the subject will find a full discussion in papers [33-34] and references wherein. In brief, the intensity of a peak hk is given by the following expression

$$I_{hk} = N m_{hk} |F_{hk}|^2 \frac{e^{-2W}}{(\sin \theta)^{3/2}} \times \left(\frac{L}{\pi^{1/2} \lambda} \right)^{1/2} \mathcal{F}(a) H(\gamma) * R(\theta) \quad (1)$$

with

$$\mathcal{F}(a) = \int_0^\infty e^{-(x-a)^2} dx$$

$$a = (2 \pi^{1/2} L / \lambda) (\sin \theta - \sin \theta_{hk})$$

$$\theta_{hk} = \sin^{-1} \lambda / 2 d_{hk} \quad \gamma = \cos^{-1} (\sin \theta_{hk} / \sin \theta)$$

where :

N is the number of unit cells of the 2D crystal ;

m_{hk} is the multiplicity of the hk th reflection ;

$F_{hk} = \sum_j b_j \exp i [2 \pi (h x_j + k y_j) + Q_\perp r_{j\perp}]$ is the

structure factor in which b_j represents the coherent scattering amplitude of the j th atom in the unit cell, x_j and y_j are its in-plane reduced positional coordinates, $r_{j\perp}$ is the component perpendicular to the surface of the interatomic vectors and Q_\perp defines the component of the scattering vector normal to the 2D lattice plane ;

e^{-2W} is the Debye-Waller factor, L is the correlation length or 2D cluster size, λ is the wavelength, d_{hk} is the 2D lattice spacing. $H(\gamma)$ defines the distribution of the preferentially orientated crystallite surfaces in the adapted Warren formalism described here. It is worth recalling that the Warren formula works only for an

isotropic distribution of planes. A more rigorous treatment for preferred orientation has been accomplished by Ruland and Tompa [43]. $H(\gamma)$ (called $F(\sigma, \varphi)$ in [43]) is actually the integrated distribution of the crystallite surfaces (more details will be published elsewhere [44]). In the present work, $H(\gamma)$ is normalized by requiring that $\int_0^{\pi/2} H(\gamma) d\gamma = 1$ and has been measured in our case by recording a rocking curve on the 01 peak of CF_4 adsorbed on papyex. It is represented in figure 5.

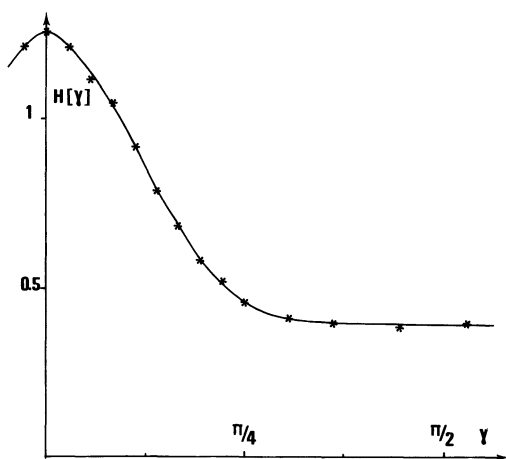


Fig. 5. — Distribution of the preferentially oriented crystallites $H(\gamma)$ obtained from the rocking curve measured on the 01 peak of CF_4 adsorbed on papyex.

$R(\theta) = (1/\Delta\pi^{1/2}) \exp(-\theta/\Delta)^2$ is the experimental Gaussian resolution of the instrument. For D1B, the width parameter Δ is 0.35° .

The intensity line profile has a sawtooth shape whose width depends on preferential orientation $H(\gamma)$, on resolution $R(\theta)$ and on cluster size L . Since the first two functions are known from experimental calibrations, the observed peak profile can be used to determine L . This point will be reported in detail in 3.2.3.

The maximum of the peak mainly depends on

$$m_{hk} \left| \sum_j b_j \exp 2\pi i(hx_j + ky_j) \right|^2 / (\sin \theta)^{3/2} \quad (2)$$

because, near the maximum, $Q_\perp \simeq 0$ and the other factors are constant like N , $(L/\pi^{1/2} \lambda)^{1/2}$, $H(\gamma)$ or nearly constant like $\mathcal{F}(a)$ and e^{-2W} . The last term is the Debye-Waller factor $W = Q^2 \langle u^2 \rangle$ where Q is the scattering vector and $\langle u^2 \rangle$ the mean square displacement of the molecule vibrations. It depends the most on θ , but our calculations are performed at 10 K a temperature where the molecules are submitted to their zero-point vibrations. This means that $\langle u^2 \rangle$ is very small and that $\exp - 2W$ is close to one.

To determine the structure, we imagine a model. The atomic positional coordinates are introduced in

(2) and the calculated relative intensities are checked against the diffraction pattern. Some hints are used to choose the model. One proceeds by analogy with the bulk structure or if the analogy does not give any result, one looks for a structure whose packing is compatible with the surface of the 2D unit cell. These ideas are developed below.

Once an agreement between the relative observed and calculated intensities is found, another test is carried out. One checks if the molecules do not overlap. This packing test is defined as follow. For every ij pairs of atoms belonging to contiguous molecules, a ratio $r_{ij}/2 R_0$ is calculated. R_0 is the mean radius of the oxygen and nitrogen atoms ($R_0 = 1.5 \text{ \AA}$) and r_{ij} is the distance between the mass centre of the i and j atoms. A realistic structure must have all its $r_{ij}/2 R_0 \geq 1$.

3.2.2.1 β solid. — The indexing of the β diffraction beams reveals systematic extinctions fulfilling the conditions $h, 0$ with $h = 2n + 1$ and $0, k$ with $k = 2n + 1$. This indicates two glide-reflection lines [35] along a and b with translation of one-half the repeat distance. Hence the 2D space group of the β solid is pgg (point group 2 mm).

The β phase is the densest 2D solid. To solve its structure, we analyse the bulk configuration of nitric oxide molecules and try to adapt this three-dimensional packing to the 2D situation. The 3D densest plane, called (001), has a rectangular cell with dimerized N_2O_2 molecules standing up almost perpendicular to this plane [36]. They obey a statistical disorder in such a way that a lattice site can be occupied with the same probability by the two configurations drawn in figure 6. Because of this disorder, a radiation see the N_2O_2 molecule in the shape of a rectangle. We keep in mind these two ideas of dimerization and statistical disorder in our investigation of the 2D adsorbed solids. In those hypothesis, each scatterer has the same coherent scattering amplitude.

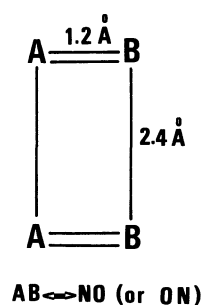


Fig. 6. — In the 2D solids, nitric oxide molecules are dimerized and exhibit a statistical disorder.

We first notice that the 2D β unit cell is very close to that of the (001) bulk plane. Furthermore, its area (25.7 \AA^2) corresponds to about twice the area of a N_2O_2 molecule standing up on its shorter side, that

is $\sim 12.6 \text{ \AA}^2$. It is reasonable to test a structure where the N_2O_2 molecules in the β phase are exactly perpendicular to the graphite surface as represented in figure 7. This model also obeys the pgg symmetry of the β phase. The only adjustable parameter is the angle \hat{i} between the molecule plane and the \mathbf{a} direction. The calculated intensities are fairly sensitive to the angle \hat{i} . The best fit between the calculated and observed relative intensities (see Fig. 3a) gives $\hat{i} = 52 \pm 10^\circ$. For this structure, the packing test always yields $r_{ij}/2 R_0 \geq 1$.

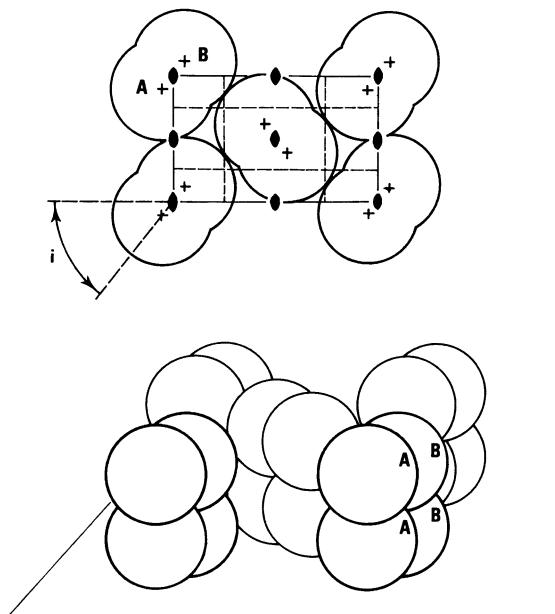


Fig. 7. — The β solid has N_2O_2 molecules standing up on the graphite substrate.

As seen in figure 7, the β crystal has a close-packed structure. The triangle formed by the mass centre of three contiguous standing up molecules is almost equilateral. This structure is similar to that of the densest plane of the bulk crystal.

The surface occupied by a molecule in the β phase ($\sim 12.8 \text{ \AA}^2$) is very close to the surface available at the layer completion (12 \AA^2). This result shows that neutron scattering measurements are compatible with our coverage calibration ($\sim 7\%$). Besides the uncertainty attached to the determination of the specific area of the substrate, there is a systematic underestimation of the area per molecule when deduced from isotherm measurements compared to diffraction analysis. The reason is that a certain amount of molecules is adsorbed on substrate defects and in the second layer as well. So the *apparent* number of molecules adsorbed in the first layer is larger than the *effective* one. It follows that the corresponding calculated area per molecule appears to be smaller than the real one deduced from the unit cell of the 2D crystal obtained from the diffraction data. The 7% difference reported

above can be partly attributed to the amount of adsorbate non located in the first layer.

3.2.2.2 γ solid. — The γ solid is stable at low coverage ($x = 0.4$). The area of the unit mesh ($\sim 21 \text{ \AA}^2$) is very close to the area of the N_2O_2 molecule parallel to its plane ($\sim 22 \text{ \AA}^2$). Hence, we interpret the different intensities in terms of a model made of rectangular molecules lying down on the graphite basal plane. Here again, the only adjustable parameter is the angle j between the large side of the rectangle and the \mathbf{a} direction. The best fit gives $j = 25 \pm 10^\circ$ yielding the structure drawn in figure 8. The calculated intensities are shown in figure 3c by arrows. This structure admits the space group $p2$.

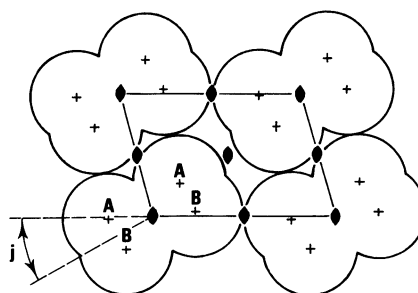


Fig. 8. — The γ solid has N_2O_2 molecules lying down on the graphite basal plane.

As for the β solid, the γ crystal has a close-packed structure but with N_2O_2 molecules lying down on the graphite surface. This packing is close to that of the (101) bulk plane.

3.2.2.3 δ solid. — The δ solid is intermediate between the β and γ phases and has a very large unit cell (see Table I). Since it occurs alone at $x = 0.65$, we can reasonably assume that this coverage corresponds approximatively to its surface saturation. Then, the δ area per molecule can be easily deduced ($12.8 \text{ \AA}^2 / 0.65$) and the number of N_2O_2 molecules in the unit cell calculated, i.e. $8.1 \times 9.5 \text{ \AA}^2 \times 0.65 / 12.8 \text{ \AA}^2 \simeq 4$. Unfortunately, the diffraction pattern does not provide enough information to solve the structure.

3.2.3 Correlation length L or 2D cluster size. — As already recalled in 3.2.2, the analysis of the line profile can yield an interesting parameter, the correlation length or 2D cluster size L . Only the diffraction pattern of the β phase exhibits a peak large enough to allow such an analysis. In fact, this peak at $2\theta \simeq 44^\circ$ is the superposition of two lines indexed 11 and 20 (Fig. 3a). The intensity I_{hk} can be calculated from (1) because the structure, i.e. $|F_{hk}|^2$ is known and the preferential orientation $H(\gamma)$ and the resolution $R(\theta)$ have been measured. Using the spectrum at 10 K, the calculation is performed a few degrees on both sides of the peak maximum, making the contribution of Q_\perp in the argument of the exponential of F_{hk} quite

negligible. We assume $N = e^{-2W} = 1$ because we only want to carry out a relative comparison. In any rate $e^{-2W} \simeq 1$ because as we said before at 10 K only the 0 point motion is to be considered and $\langle u^2 \rangle \simeq 0$. By choosing $L = 250 \text{ \AA}$ (and $m_{11} F_{11}^2 = 1$; $m_{20} F_{20}^2 = 0.4$; $m_{21} F_{21}^2 = 0.25$ given by the structure), we get the theoretical curves represented in figure 9. The maximum of I_{hk} was chosen in such a way that it corresponds to the maximum of the measured intensity at $2\theta \simeq 44^\circ$.

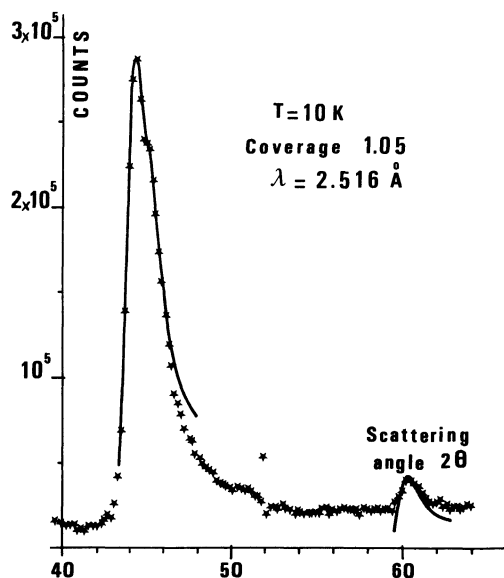


Fig. 9. — Fitted peak shapes for the β solid (see § 3.2.3).

The agreement between the calculated and measured line profiles is fairly good. The theoretical curves fit well the main features of the data like the general shape, the position in 2θ , the shoulder at 45° (indication of the 20 Bragg peak), the 21 peak whose intensity is not adjusted and the line width as well. But the calculated intensity is too large above $46-47^\circ$ and too small above 61° . The first defect cannot be rectified by increasing L because this would contract the 21 peak which is already too narrow. This slight discordance between the observed and calculated trailing edge of the diffraction line shows the limitation of the analysis through the framework of Warren-Kjems formalism. It could be due to the fact that the peak at 45° is the superposition of two diffracted lines. Any small variation of the maximum line positions will produce a change in the peak shape. We did not try to introduce a new parameter in our fit.

The value $L \simeq 250 \text{ \AA}$ seems to characterize the mean size of the 2D adsorbed islands on papyx. It was already found for the cluster size of Kr [31] and CD_4 [25] adsorbed on this substrate. Another recompressed graphite powder (see § 2), called grafoil [15, 16, 33] is often used in neutron studies of adsorbed layers. Both substrates have comparable specific areas, preferential orientations and densities. The mean value of L

for grafoil is about 100 \AA . One can conclude that papyx is better than grafoil as far as the size of the diffracting arrays is concerned.

We could also note that another form of graphite powder called UCAR-ZYX has a larger mean size [42] ($\sim 500 \text{ \AA}$). However, its specific surface is smaller than papyx or grafoil. The adsorbed scatterers are reduced and this substrate seems inappropriate for diffraction studies with the weak neutron fluxes.

3.2.4 Mean squared displacements and thermal expansion. — The β phase is stable within a temperature range of 64 K between 10 K and 74 K. The intense peak at 44° indexed 11 (Fig. 3a) allows us to determine two thermal properties, i.e. the variation of the mean squared displacement $\langle u^2 \rangle$ of the N_2O_2 molecules from the Debye-Waller factor and the mean coefficient of thermal expansion from the variation of the position of the peak between 10 K and 74 K. Two spectra have been measured at 10 K and 74 K. $\langle u^2 \rangle$ parallel to the surface has been calculated with respect to the value (unknown but close to 0) at 10 K. The results indicate $\Delta \langle u^2 \rangle \simeq 0.02 \text{ \AA}^2$. It is worth noticing that for bulk NO $\langle u^2 \rangle \simeq 2.5 \times 10^{-2} \text{ \AA}^2$ at $T = 98 \text{ K}$ [37] which is an average value determined from the temperature factor. So, the mean squared displacements of N_2O_2 dimers have about the same value in the β solid phase that in the bulk. It is not surprising if we remember that the distance between molecule in the β phase is about the same that in the (001) plane of bulk NO. However, we must be aware that any temperature dependence in the atomic positional parameters within the unit cell would also contribute to change in intensity.

When T changes, the position of the Bragg peaks moves a little. It gives us a mean to measure the average thermal expansion coefficient between 10 K and 74 K along a and b directions. We found

$$\frac{1}{\Delta T} \frac{\Delta a}{a} \simeq 2.3 \times 10^{-4} \text{ K}^{-1}$$

and

$$\frac{1}{\Delta T} \frac{\Delta b}{b} \simeq 1 \times 10^{-5} \text{ K}^{-1}.$$

The values are smaller than that found for Ar by Taub *et al.* [15] which is $\simeq 1.5 \times 10^{-3} \text{ K}^{-1}$, or that found by Venables *et al.* [5] for Xe which is $\simeq 3 \times 10^{-3} \text{ K}^{-1}$. Typical values are $\simeq 3 \times 10^{-4} \text{ K}^{-1}$ for bulk argon, $\simeq 9 \times 10^{-4}$ for bulk xenon which are smaller than the corresponding 2D ones. This is certainly due to the lower dimensionality of the system where molecules have less neighbours. Unfortunately we don't know the value for bulk nitric oxide.

4. Melting and 2D fluids. — We investigated thoroughly the thermal stability of the solids γ , δ , β . A detailed description will be given in 5. In this section, we indicate what the diffraction can bring for the understanding of 2D fluids.

Typical Debye-Scherrer spectra of NO 2D fluids are given in figure 10a, b, c for various coverages and temperatures. From the thermodynamic study of MTD, we know that at 98 K, the layer is in a hypercritical state. The scattered intensity gives a broad peak whose amplitude depends on coverage (Figs. 10a and 10b). Its width can be characterized by a correlation length of $\sim 8 \text{ \AA}$, obtained by using the Scherrer formula. This value is only an order of magnitude deduced from an approximate theory. Its main interest is to show that the correlation length is 2D fluids is clearly smaller than in 2D solids.

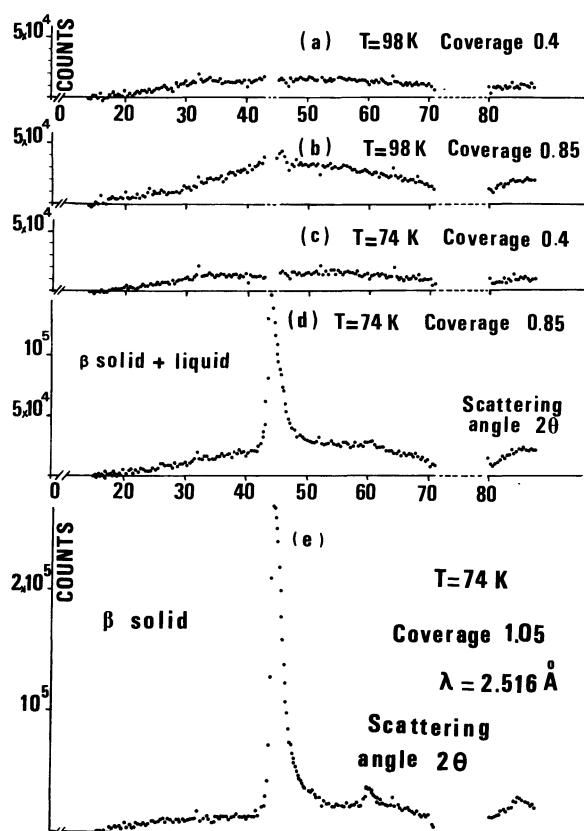


Fig. 10. — Neutron scans at 98 K and 74 K and various coverages. Graphite background has been subtracted (see caption of figure 3). a) and b) 2D hypercritical phase, $T = 98 \text{ K}$ and coverage = 0.40 and 0.85 respectively; c) 2D liquid-gas coexistence, $T = 74 \text{ K}$, coverage = 0.40; d) 2D liquid- β solid coexistence, $T = 74 \text{ K}$, coverage = 0.85. This is the signature of a 2D first order melting transition; e) 2D β solid phase, $T = 74 \text{ K}$, coverage = 1.05

When the temperature is decreased at 74 K, at constant coverage, the spectrum does not change for $x = 0.4$ (Fig. 10c), whereas it is completely modified for $x = 0.85$ (Fig. 10d). According to the MTD study, at $x = 0.4$, $T = 74 \text{ K}$, we are in the coexistence domain gas $2D \rightleftharpoons \alpha$ phase and at $x = 0.85$, $T = 74 \text{ K}$, in the domain $\alpha \rightleftharpoons \beta$. One immediately sees that the α phase is a 2D liquid for the contribution of the 2D gas to the scattered intensity is quite negligible. We should find again in figure 10d (coverage 0.85) a

mixture of liquid and β solid. We do observe the peak at $2\theta = 44^\circ$ characteristic of the β phase, but the liquid is less obvious to detect for it should give rise to a broad peak superimposed to the narrow peak from the β crystal. We can show that it exists if we compare the diffraction spectrum of figure 10e obtained at the same temperature for $x = 1.05$ to the spectrum of figure 10d. At $x = 1.05$, β appears alone. If at $x = 0.85$ there was only β solid, we should expect the peak at 44° reduced by an amount proportional to the decrease in x , i.e. $\sim 20\%$. Actually, the intensity of the peak has decreased by a factor two. So, the layer is not formed only by the β solid. Furthermore, the background is slightly larger (see for instance around $2\theta = 40^\circ$) in figure 10d. This increase of the main peak wings can be attributed to the existence of a liquid. We estimate that half the surface is occupied by the β solid, the other half being occupied by the α liquid. As a matter of fact, if we superimpose figures 10c ($x = 0.4$; $T = 74 \text{ K}$) and 10e ($x = 1.05$; $T = 74 \text{ K}$) weighed by the relative amounts of liquid and solid, we obtain the spectrum of figure 10d. This observation of the coexistence of 2D liquid and 2D solid is very important; it shows that the β crystal melts in a first order transition. It should be pointed out that the observation of a two phase coexistence in a neutron experiment could be fortuitous if heterogeneities are present. However, in our case, the gradient of chemical potential determined along the step of the adsorption isotherm (§ 2) is not strong enough to account for such an effect.

As we mentioned in the introduction, the problem of the order of the 2D melting transition has been raised since many years. A rule had been proposed by experimentalists [1]. The melting transition would be first order if the 2D crystal structure is commensurate with the substrate and higher order otherwise. The present results show that this rule does not hold for the β crystal is not commensurate with the graphite surface.

Theorists investigated the mechanism of 2D melting. The Kosterlitz-Thouless model is based on the ideas that a 2D crystal melts through the dissociation of dislocation pairs [10, 38]. Nelson and Halperin (N. H.) argue that the new melted phase is a new kind of liquid crystal [11]. Translational order decays exponentially but orientational order persists above T_m with bond angle correlations decaying to zero. So the melting occurs in a two stage second order transition. N. H. does not rule out the possibility of first order melting transition. They also investigate the effect of a periodic substrate on their theory of melting and distinguish between commensurate and floating solids. It comes out that no general rule can be set up to predict *a priori* the nature of the melting transition in a real system and a lot remains to do in that domain.

5. Phase diagram. — About thirty diffraction patterns have been measured between 10 and 98 K

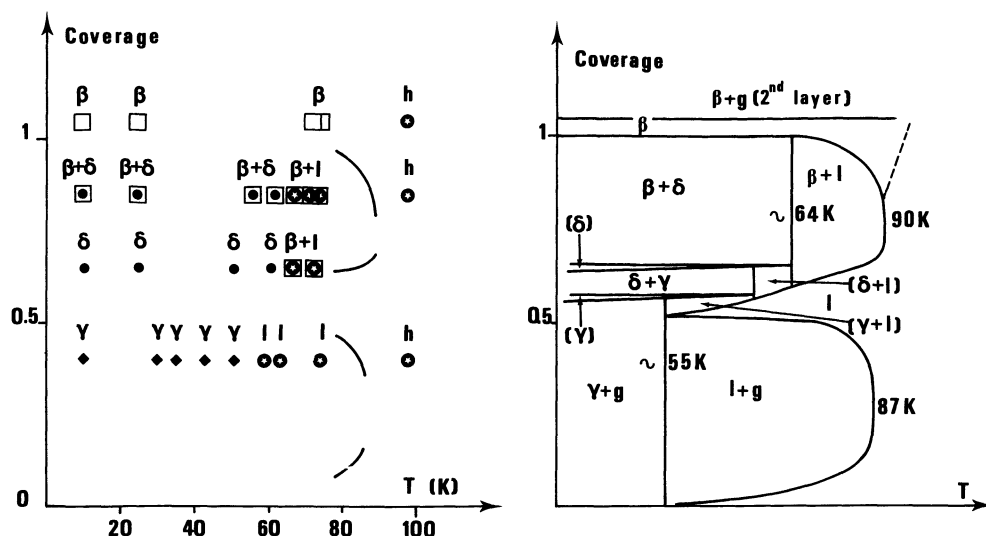


Fig. 11. — Neutron scattering and adsorption isotherm results as a function of coverage and temperature (Fig. 11a) and tentative schematic phase diagram featuring in particular three triple points, one critical temperature and one tricritical point (Fig. 11b). Three solids β , γ , δ , one liquid $l = \alpha$ and one hypercritical phase h have been observed.

(Fig. 11a). They display the characteristic lines of the β , γ and δ solids or the broad peak of the α liquid. In a few cases they exhibit, as explained previously, the superposition of the diffraction features of two different phases, indicating a coexistence between two solids or between a solid and a liquid. The results show that the γ and δ solids alone are stable up to 50.5 and 61 K respectively. The coexistence between β and δ at $x = 0.85$ disappears above 62 K and is replaced at 67 K by a mixture of β and α liquid. At $x = 1.05$, the β solid melts at about 98 K because the diffraction pattern exhibits an intense broad peak overtopped by a small residual β peak. This observation is trouble some for the tricritical point of the β -liquid transition is close to 90 K [27]. The melting transition should be continuous and the β -liquid coexistence should not be observed at 98 K. It is possible that the small quantity of β phase detected on the diffraction pattern can be stabilized by heterogeneities.

All the experimental results, including the MTD gas-liquid and liquid- β phase limits, have been reported in figure 11a. These raw data can be analysed a little deeply in considering the previous structural and thermodynamic conclusions. Knowing the surface of a lying-down molecule ($\sim 21 \text{ \AA}^2$), one can calculate at $x = 0.4$ the relative surface occupied by the γ solid on the graphite surface. The value

$$\frac{21 \text{ \AA}^2}{12 \text{ \AA}^2/0.4} \sim 0.7$$

indicates that a free space keeps the 2D γ crystals apart. It is reasonable to assume that this available surface is filled with a 2D gas. Furthermore, a 2D liquid is observed at $x = 0.4$ and $T = 59, 63, 74 \text{ K}$. The thermodynamic study of MTD showed that this condensed phase coexisted with a dilute phase which

was the 2D gas as well. Summarizing the neutron scattering and adsorption isotherm measurements, four first order phase transitions, namely β solid \rightleftharpoons δ solid, β solid \rightleftharpoons α liquid, γ solid \rightleftharpoons gas and α liquid \rightleftharpoons gas, have been observed in the first layer of nitric oxide adsorbed on (0001) graphite.

The results represented figure 11a and the above discussion permit to propose a tentative phase diagram drawn in figure 11b. The phase boundaries are not very well-known and we did not try to plot it precisely. In fact, we exaggerated some phase domains for the sake of clarity. The coverage scale is approximately respected but the temperature coordinate is expanded between 55 and 64 K. A few reference marks are given to compare easily figures 11a and 11b. This proposed phase diagram indicates that the nitric oxide adsorbed layer has three triple points (liquid-gas- $\gamma \sim 55 \text{ K}$; γ -liquid- δ ; δ -liquid- $\beta \sim 64 \text{ K}$), one critical temperature $\simeq 87 \text{ K}$ and one tricritical point $\simeq 90 \text{ K}$. Hence a simple molecule like nitric oxide can display a fairly complex two-dimensional phase diagram which is unquestionably much richer than that of the bulk. The reduction of dimensionality and the substrate field induce various molecules configurations whose stability domains extend on a few tens of degrees.

6. Discussion and conclusion. — Three 2D solids γ , δ and β have been found in the first layer of NO adsorbed on graphite. Two structures γ and β have been solved. They are formed of N_2O_2 dimers lying down or standing up on the substrate. Those models fit very well the diffraction intensities but we are aware that other techniques (LEED, energy loss spectroscopy...) could bring extra information and help to precise the proposed models and to determine the structure of the δ phase.

All the solid unit cells are incommensurate with

the graphite basal plane. But we cannot rule out any superlattice involving a long range epitaxial relation. Only a diffraction study on a single crystal surface, by electron diffraction for instance, could solve the question. Such measurement could also provide information about the orientation of the adsorbed layer with respect to the substrate lattice [4, 5].

The mechanism by which the N_2O_2 molecules are going from their lying-down position (γ) to their standing up configuration (β) is unknown. But we showed it occurs *via* an intermediate phase (δ). The

coexistence between the δ and β phases suggests that the transition δ - β is first order.

This study shows the ability of neutron scattering technique to solve questions that adsorption volumetry measurements leave open and to bring new information on 2D adsorbed phases. In the case of NO besides the different solid structures, we determine the nature of the α phase which is a 2D liquid, and we rule out the hypothesis of a triple point at 15 K. Finally we showed that the melting of the β phase is a first order transition.

References

- [1] DASH, J. G., *Films on Solid Surfaces* (Academic Press, New York) 1975.
- [2] Two-dimensional adsorbed phases, *J. Physique Colloq.* **38** (1977) C4.
- [3] *Phase transitions in Surface Films*, Ed. Dash J. G. and Ruwals J. (Plenum Press) 1980, to be published.
- [4] FAIN, S. C. and CHINN, M. D., in [2], p. 99.
- [5] VENABLES, J. A. and SCHABES-RETKHIMAN, P. S., in [2], p. 105.
- [6] McTAGUE, J. P. and NIELSEN, M., *Phys. Rev. Lett.* **37** (1976) 596.
- [7] ECKERT, J., ELLENSON, W. D., HASTINGS, J. B. and PASSELL, L., *Phys. Rev. Lett.* **43** (1979) 1329.
- [8] COULOMB, J. P., BIBERIAN, J. P., SUZANNE, J., THOMY, A., TROTT, G. J., TAUB, H., DANNER, H. R. and HANSEN, F. Y., *Phys. Rev. Lett.* **43** (1979) 1878.
- [9] SUZANNE, J., COULOMB, J. P., MATECKI, M., THOMY, A., CROSET, B. and MARTI, C., *Phys. Rev. Lett.* **41** (1978) 760.
- [10] HOLZ, A. and MADEIROS, J. T. N., *Phys. Rev. B* **17** (1978) 1161.
- [11] NELSON, D. R. and HALPERIN, B. I., *Phys. Rev. B* **5** (1979) 2457.
- [12] DOMANY, E., SCHICK, M., WALKER, J. S. and GRIFFITHS, R. B., *Phys. Rev. B* **18** (1978) 2209.
- [13] BRETZ, M., DASH, J. G., HICKERNELL, D. C., McLEAN, E. O. and VILCHES, O. E., *Phys. Rev. A* **8** (1973) 1589; *A* **9** (1974) 2814.
- [14] HUFF, G. B. and DASH, J. G., *J. Low Temp. Phys.* **24** (1976) 155.
- [15] TAUB, H., CARNEIRO, K., KJEMS, J. K., PASSELL, L. and McTAGUE, J. P., *Phys. Rev. B* **16** (1977) 4551.
- [16] NIELSEN, M., McTAGUE, J. P. and ELLENSON, W., in [2], p. 10.
- [17] MARLOW, I., THOMAS, R. K., TREWERN, T. D. and WHITE, J. W., in [2], p. 19.
- [18] GRILLET, Y., ROUQUEROL, F. and ROUQUEROL, J., in [2], p. 57.
- [19] SUZANNE, J. and BIENFAIT, M., in [2], p. 82.
- [20] CHUNG, T. T., *Surf. Sci.* **87** (1979) 348.
- [21] SHECHTER, H., SUZANNE, J. and DASH, J. G., *Phys. Rev. Lett.* **37** (1976) 706.
- [22] CHUNG, T. T. and DASH, J. G., *Surf. Sci.* **66** (1977) 559.
- [23] LARHER, Y., *J. Chim. Phys.* **68** (1978) 2257.
- [24] BUTLER, D. M., LITZINGER, J. A., STEWART, G. A. and GRIFFITHS, R. L., *Phys. Rev. Lett.* **42** (1979) 1289.
- [25] GLACHANT, A., COULOMB, J. P., BIENFAIT, M. and DASH, J. G., *J. Physique Lett.* **40** (1979) 1-543.
- [26] WIDOM, A., OWERS-BRADLY, J. R. and RICHARDS, M. G., *Phys. Rev. Lett.* **43** (1979) 1340.
- [27] MATECKI, M., THOMY, A. and DUVAL, X., *J. Chim. Phys.* **71** (1974) 1484.
- [28] MATECKI, M., THOMY, A. and DUVAL, X., *Surf. Sci.* **75** (1978) 142.
- [29] Papyex is the trade name of the product of Carbone Lorraine, 37-41 rue Jean-Jaurès, 92231 Gennevilliers (France).
- [30] COULOMB, J. P., BIENFAIT, M. and THOREL, P., in [2], p. 31.
- [31] CEVA, T. and MARTI, C., *J. Physique Lett.* **39** (1978) L-221.
- [32] COULOMB, J. P., BIENFAIT, M. and THOREL, P., *Phys. Rev. Lett.* **49** (1979) 733.
- [33] KJEMS, J. K., PASSELL, L., TAUB, H., DASH, J. G. and NOVACO, A. D., *Phys. Rev. B* **13** (1976) 1446.
- [34] WARREN, B. E., *Phys. Rev.* **59** (1941) 693.
- [35] *International tables for X-Ray Crystallography* (The Kynoch Press, Birmingham) 1965.
- [36] WYCKOFF, R. W. G., *Crystal Structures* (Wiley London) 1963, Vol. 1.
- [37] DULMAGE, W. J., MEYERS, E. A. and LIPSCOMB, W. N., *Acta Crystallogr.* **6** (1953) 760.
- [38] KOSTERLITZ, J. M. and THOULESS, D. J., *J. Phys. C* **5** (1972) 124; *C* **6** (1973) 1181.
- [39] OSTLUND, S. and BERKER, A. N., *Phys. Rev. Lett.* **42** (1979) 843.
- [40] LARHER, Y., *J. Chem. Phys.* **68** (1978) 2257.
- [41] LARHER, Y. and TERLAIN, A., *J. Chem. Phys.* **72** (1980) 1052.
- [42] STEPHENS, P. W., HEINEY, P., BIRGENEAU, R. J. and HORN, P. M., *Phys. Rev. Lett.* **43** (1979) 47.
- [43] RULAND, W. and TOMPA, H., *Acta Crystallogr. A* **24** (1968) 93.
- [44] COULOMB, J. P., BIENFAIT, M. and THOREL, P., *J. Physique* (to be published).